www.czasopisma.pan.pl PAN POLSKA AKADEMIA NAUK www.journals.pan.pl

Arch. Metall. Mater. **64** (2019), 2, 791-796

DOI: 10.24425/amm.2019.127615

K. GRANEK*#, G. ZIÓŁKOWSKI*, A. CHROBAK*, J. KLIMONTKO*,
J. RAK**, O. ZIVOTSKY***, L. GEMBALOVA***

ULTRA-FAST CURRENT AIDED SINTERING OF HIGH COERCIVE MAGNETIC POWDERS AND COMPOSITES

The paper refers to pulverization and sintering of the $(Fe_{80}Nb_6B_{14})_{0.88}Tb_{0.12}$ high coercive alloy. The powder was sintered using the ultra-fast current aided method. It turned out that too long discharge time leads to appearing of a soft magnetic phase and simultaneously, decrease in coercivity of the compacted powder. Nevertheless, it was possible to establish preference technology parameters, preserving magnetic hardness of the alloy. As a final test, an impact of Co-powder addition on magnetic properties was studied. The introduced soft magnetic phase (about 20 wt. %) caused about 30% increase of magnetic remanence, which is a result of direct exchange interactions between the two phases.

Keywords: magnetic composites, ultra-fast current sintering, high coercive alloys

1. Introduction

Magnetic materials are very important in nowadays technologies [1,2]. New and continuously increasing requirements can be fulfilled by modern nanostructured magnetic composites containing phases characterized by different magnetic properties [3-7]. Recently, we reported ultra-high coercivity (>7 T) in Fe-Nb-B-Tb type of bulk nanocrystalline alloys prepared by the vacuum suction casting technique [8,9]. It was shown that in such materials the interactions between relatively soft ($TbFe_2$) and hard magnetic phases ($Tb_2Fe_{14}B$) with specific irregular branches are especially important and can lead to appearing of new and unique properties. On the other hand, the antiferromagnetic coupling between Fe and Tb limits the maximum of magnetic saturation and, as a consequence, reduces the application potential for such materials. However, alloys with ultra-high coercivity may be a key element for the composites containing also some soft magnetic phases (like Fe or Co) and via the interactions with their surrounding can lead to improvement of the magnetic remanence of the composite. One of possible ways to obtain such composites containing interacting magnetically hard and soft phases is grinding and sintering of the materials. The first point was reported by us [10] with the conclusion that micrometric grains of the $(Fe_{80}Nb_6B_{14})_{0.88}Tb_{0.12}$ alloy preserve it's high coercivity while further pulverization leads to significant deterioration of the hard magnetic properties. Compacting the studied powder by typical heating methods can not be used because of destroying its microstructure as well as iron separation that both leads to undesirable magnetic softening. Therefore, the spark plasma sintering technique was used in order to omit the mentioned problems.

The aim of the paper is to study an influence of ultra-fast current aided sintering on structural and magnetic properties of the $(Fe_{80}Nb_6B_{14})_{0.88}Tb_{0.12}$ micrometric powder. Additionally, the composite consisting of $(Fe_{80}Nb_6B_{14})_{0.88}Tb_{0.12}$ plus Co powders was investigated.

2. Experimental procedure

The powder of the $(Fe_{80}Nb_6B_{14})_{0.88}Tb_{0.12}$ alloy was prepared in the two steps: i) the bulk rod of the $(Fe_{80}Nb_6B_{14})_{0.88}Tb_{0.12}$ alloy was obtained by the vacuum suction technique in the form of rods with 1 mm in diameter [11], ii) the rods were crushed by means of the low energy ball mill (15 min). Further, the obtained powder was compacted with the use of the self designed ultra-fast current aided sintering apparatus, as shown in Fig. 1. Table 1 describes selected conditions used in the sample preparation (capacitance C, voltage V_Z, estimated discharging time t_D and the energy E absorbed in the sample during the capacitor discharging). As a final test, samples composed of $(Fe_{80}Nb_6B_{14})_{0.88}Tb_{0.12}$ powder with addition of Co powder were prepared. The Co content in these samples was equal to 4.74 wt. %, 9.06 wt. %, 20.98 wt. % and 27.1 wt. %, and in the text they are denoted as Co_5, Co_10, Co_20 and Co_25, respectively.

* UNIVERSITY OF SILESIA, INSTITUTE OF PHYSICS, 75 PUŁKU PIECHOTY 1A, 41-500 CHORZÓW, POLAND
** UNIVERSITY OF SILESIA, INSTITUTE OF MATERIALS SCIENCE, 75 PUŁKU PIECHOTY 1A, 41-500 CHORZÓW, POLAND
*** VŠB – TECHNICAL UNIVERSITY OF OSTRAVA, DEPARTMENT OF PHYSICS, 17. LISTOPADU 15/2172, 708 33 OSTRAVA-PORUBA, CZECH REPUBLIC
# Corresponding author: krzysztof.granek@gmail.com

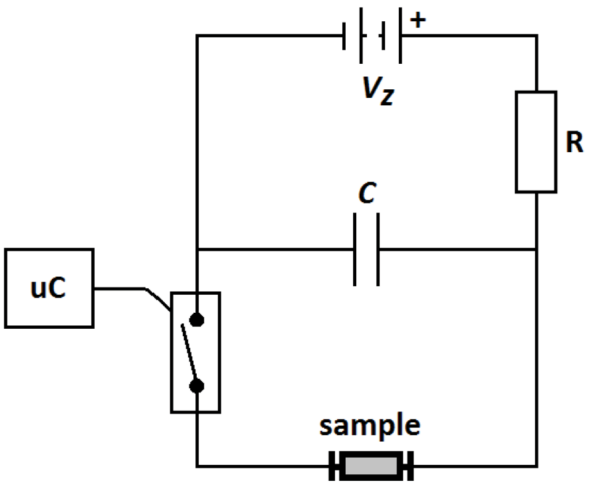

Fig. 1. Simplified scheme of the ultra-fast current aided sintering aparatus

TABLE 1

Selected conditions used during sample preparation – capacitance C, voltage V_Z, estimated discharging time t_D and the energy E absorbed in the sample during the capacitor discharging

C (μF)	V_Z (V)	t_D (μs)	E (J)
200	200	300	4
200	300	300	9
200	400	300	36
50	300	75	2.25
50	400	75	4
50	500	75	6.25
10	800	15	3.2
10	1000	15	5
10	1200	15	7.2
10	1600	15	12.8

Structural properties were determined by means of XRD (PANalytical Empyrean diffractometer with Cu Kα radiation (40 kV, 30 mA) equipped with a PIXcel detector) as well as SEM (Scanning Electron Microscope FEI Quanta 650 FEG, Acceleration voltage: 10 kV, Current: 8-10 nA, Pressure in vacuum chamber: 50 Pa) techniques. A phase structure of the tested composites was determined using the X'Pert High Score Plus program which is based on the RIR (Reference Intensity Ratio) values.

Magnetic hysteresis loops were measured using SQUID magnetometer (XL-7 MPMS system, Quantum Design).

3. Results and discussion

Magnetic parameters of the obtained samples were determined from hysteresis loops measured at the room temperature and ±7 T external magnetic field. Figs. 2, 3 and 4 show the hysteresis for the powders of $(Fe_{80}Nb_6B_{14})_{0.88}Tb_{0.12}$ sintered with C = 200 μF, 50 μF and 10 μF (different discharge time), respectively. Additionally, V_Z varied from 200 V to 1600 V in order to increase energy absorbed by the samples.

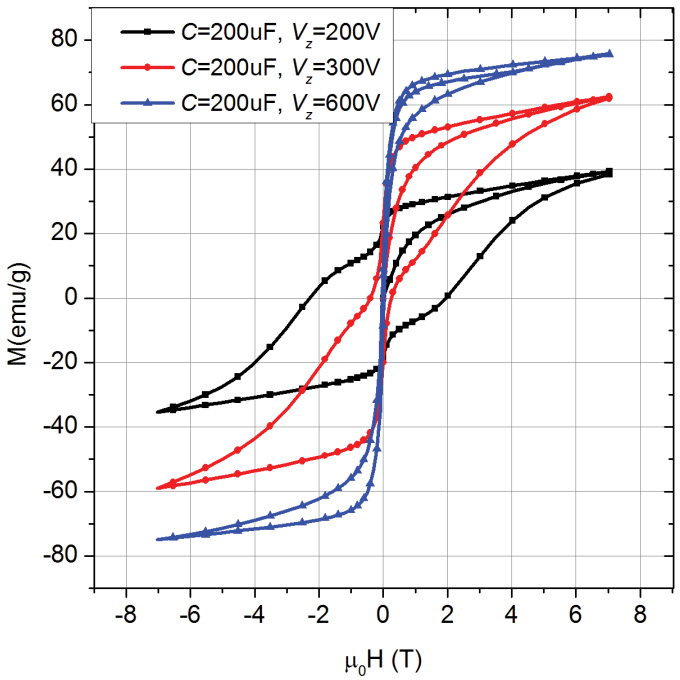

Fig. 2. Hysteresis loops for the samples sintered with C = 200 μF and different volatges

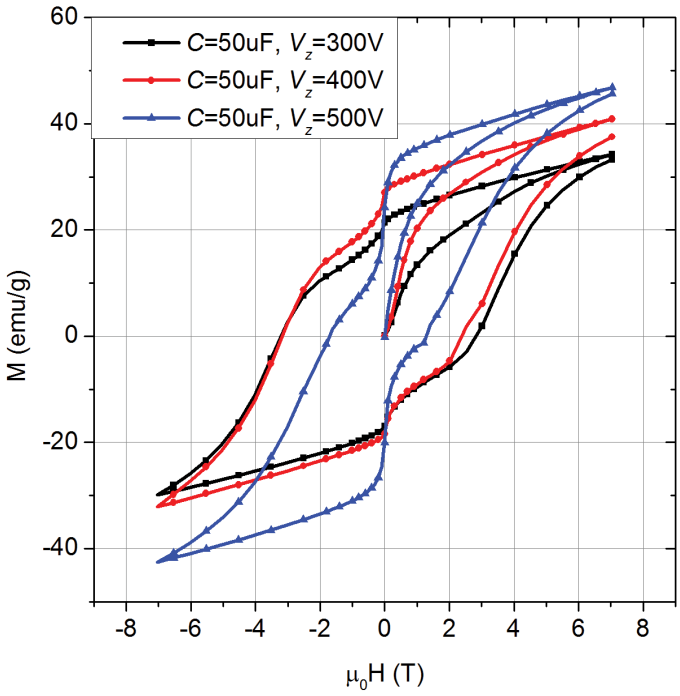

Fig. 3. Hysteresis loops for the samples sintered with C = 50 μF and different volatges

As shown, in all examined cases the hysteresis loops consist of the two components: i) magnetically soft – the magnetization jump near $\mu_0 H$ = 0 T and ii) magnetically hard – the maximum magnetization slope in the fields about ±3 T. Moreover, the common tendency is the increase of the soft component contribution with the increase of V_Z which is related to the energy stored in the capacitor. Similarly, the magnetic saturation gradually increases with the increasing contribution of the soft component.

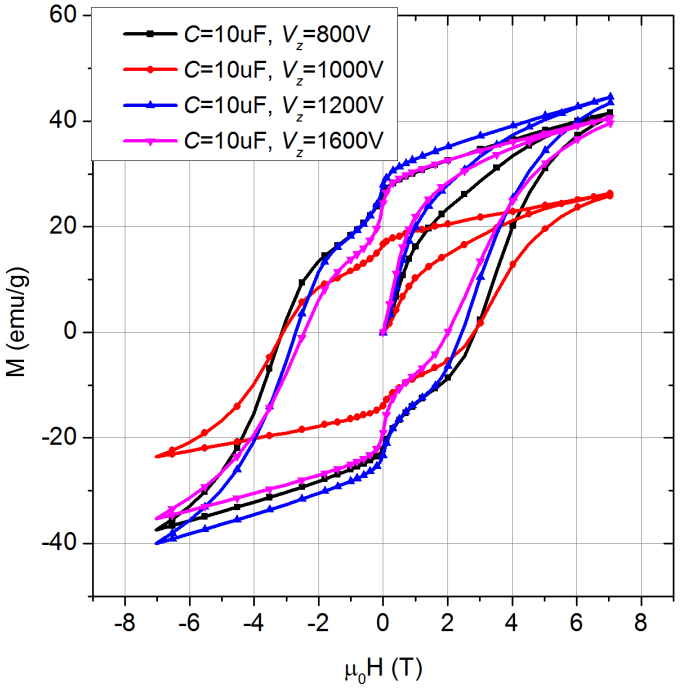

Fig. 4. Hysteresis loops for the samples sintered with C = 10 μF and different volatges

It is worth to compare the hysteresis loops for samples with similar absorbed energy and different discharge time. Fig. 5 depicts such a comparison for the energy about 7 J. The change of the capacitance C is related to the change of the current impulse time during the discharging. For resistance of the samples equal about 0.5 Ω, this time varied from 15 μs to 300 μs for C ranging from 10 μF to 200 μF. Comparing the hysteresis presented in Fig. 5, one may conclude that the shortening of the discharge

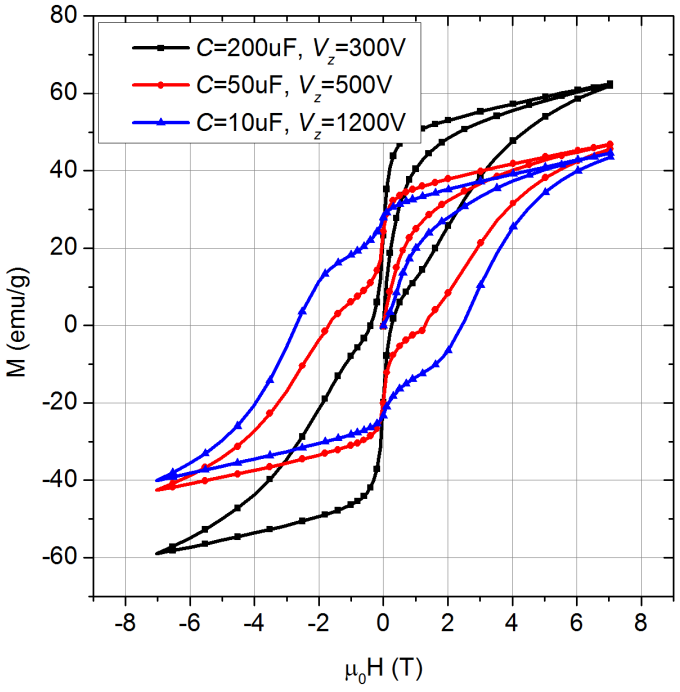

Fig. 5. Hysteresis loops for the samples with the absorbed energy equal to about 7 J

time results in preserving hard magnetic properties of the compacted powder. In other words, to long discharge time leads to undesired magnetic softening.

The effect can be explained by the structural investigations. Fig. 6 shows the XRD patterns for the samples with the absorbed energy equal to about 7 J. The determined phase contents are listed in Table 2. Analyzing the results, one can state that the increasing discharging time causes the observed decrease of the $Tb_2Fe_{14}B$ hard magnetic phase from 86 wt. % to 76 wt. % for $t \approx 15$ μs (C = 10 μF) to $t \approx 300$ μs (C = 200 μF). The other appearing phases (Fe, Fe_2Tb,$TbFe_3$) are magnetically soft, and therefore, are responsible for the deterioration of the hard magnetic properties. This means that "overheating" the

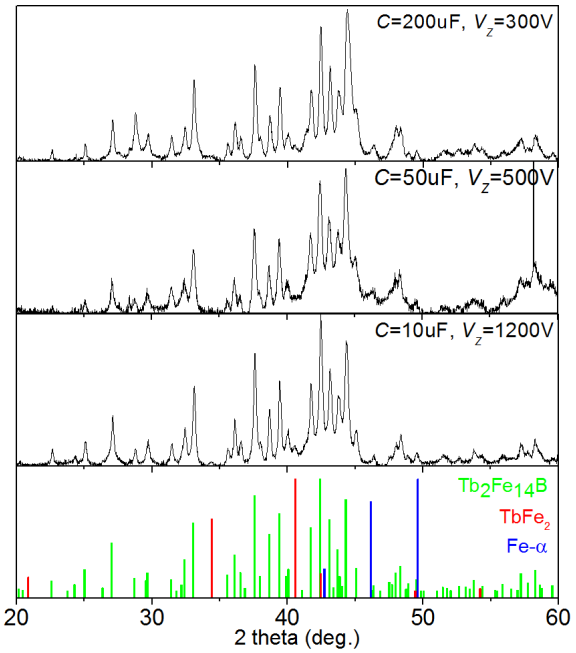

Fig. 6. XRD patterns for the samples with the absorbed energy equal to about 7 J

TABLE 2

Determined phase contents for the samples with the absorbed energy equal to about 7 J. C denotes capacity and V_Z denotes voltage used during sample preparation

Sintering conditions	Phase	Phase content [wt. %]
C = 200 μF V_Z = 300 V	Tb2Fe14B	76
	TbFe3	7
	Fe	8
	other (eg. Tb2O3, Tb11O20)	9
C = 50 μF V_Z = 500 V	Tb2Fe14B	82
	TbFe3	8
	Fe	4
	other	6
C = 10 μF V_Z = 1200 V	Tb2Fe14B	86
	TbFe3	5
	Fe	3
	Fe2Tb	3
	other	3

grains destroys the original ultra-high coercive phase and the efficient sintering should melt only intergrain surface. Due to the finite thermal conductivity of the powder, it is possible only by extremely short discharging time and voltage high enough, ensuring proper energy to compact the sample.

This conclusions can be confirmed and emphasized by the performed SEM observations. Figs. 7, 8 and 9 depict the SEM images (in the back scatter electron mode) for the samples sintered with the use of $C = 200$ µF, 50 µF and 10 µF, respectively.

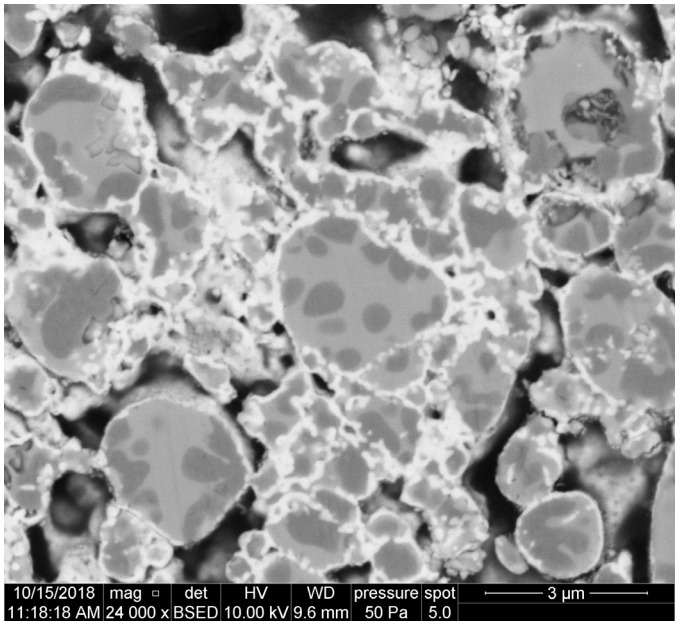

Fig. 7. SEM picture for the sample sintered with C = 200 µF and V_Z = 300 V

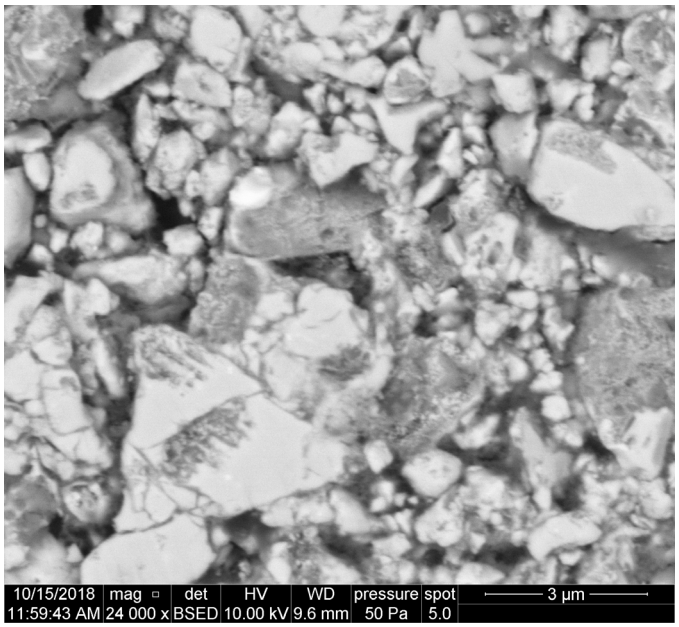

Fig. 8. SEM picture for the sample sintered with C = 50 µF and V_Z = 500 V

In the case of $C = 200$ µF, the grains are quite well bonded, however, the visible chemical contrast inside the grains indicates

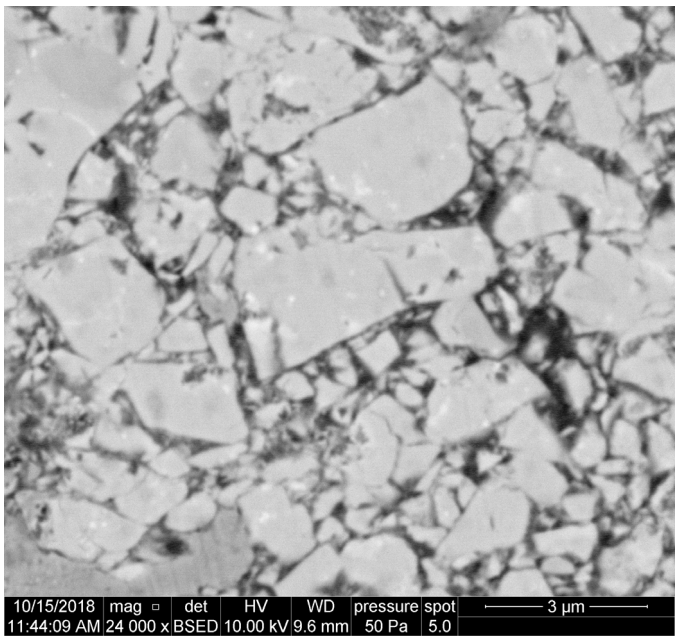

Fig. 9. SEM picture for the sample sintered with C = 10 µF and V_Z = 1200 V

the phase changes attributed to appearing of the magnetically soft phases observed in the XRD measurement (see Table 2). For the remaining cases, the intergrain bonding is not as effective as for the longest discharging time but the grains are chemically unchanged, especially when C =10 µF.

Finally, among the studied range the best technology conditions were established as C = 10 µF and V_Z = 1200 V. For this selection a set of powder composites, consisting of the hard magnetic $(Fe_{80}Nb_6B_{14})_{0.88}Tb_{0.12}$ and soft magnetic Co powders was sintered. The Co concentration varied in the range from about 5 to 25 wt. %. An example of microstructure (SEM and EDS) for the sample with 20 wt. % of Co is depicted in Fig. 10.

The EDS Co map clearly indicates the Co grains. Maps of Fe and Tb coincidence with the Co one, showing occurrence of the hard magnetic $(Fe_{80}Nb_6B_{14})_{0.88}Tb_{0.12}$ phase.

Fig. 11 shows the so-called remagnetization curves, i.e. magnetization vs. magnetic field changing from +7 T to –7 T.

Generally, with the increase of the Co content, one can see the increase of the magnetic saturation accompanied by the observed decrease of coercivity as well as significant increase of the soft component contribution (see the magnetization change near zero field). Selected magnetic parameters like magnetic saturation M_s, magnetic remanence M_r and coercive field H_c in a function of Co content are depicted in Fig. 12. In order to avoid some irreversible effects, characteristic for magnets with ultra-high coercive phases, the magnetic saturation was determined in the third quadrant of the remagnetization curves, i.e. after the first saturation.

As it was expected, the magnetic saturation linearly increases with the increasing amount of the Co powder. The other parameters M_r and H_c decrease with the increase of the Co concentration, but, one can notice a singularity about 20 wt. % of Co. In fact, these quantities unexpectedly increases (e.g. M_r

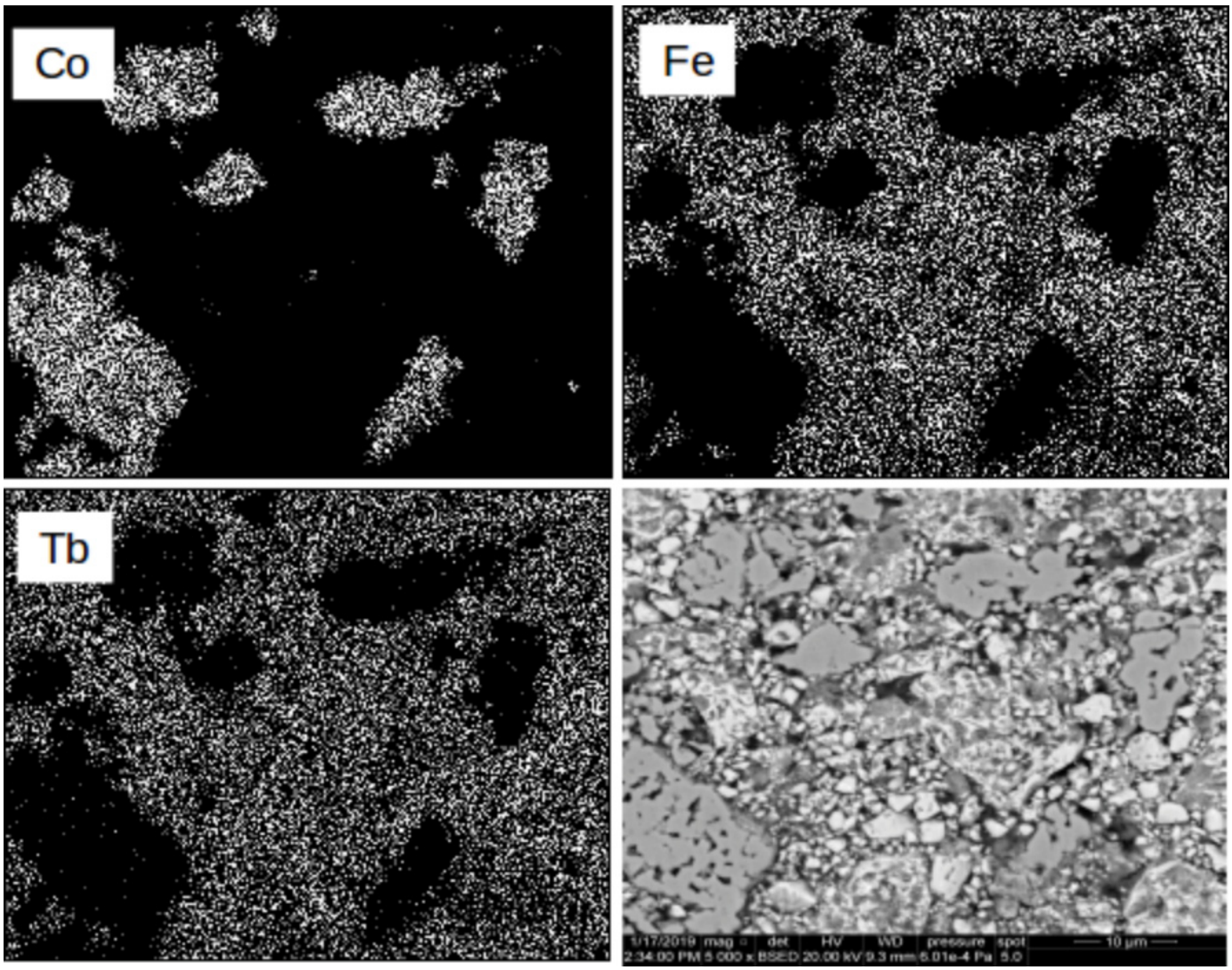

Fig. 10. EDS maps and SEM (BSE mode) picture for the sample with 20 wt. % of Co powder

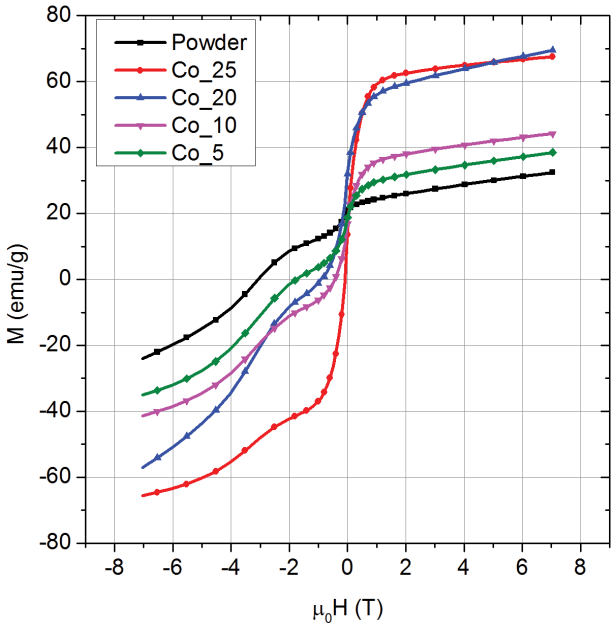

Fig. 11. Remagnetization curves for composites consisting of the hard magnetic $(Fe_{80}Nb_6B_{14})_{0.88}Tb_{0.12}$ and different amount of soft magnetic Co powders

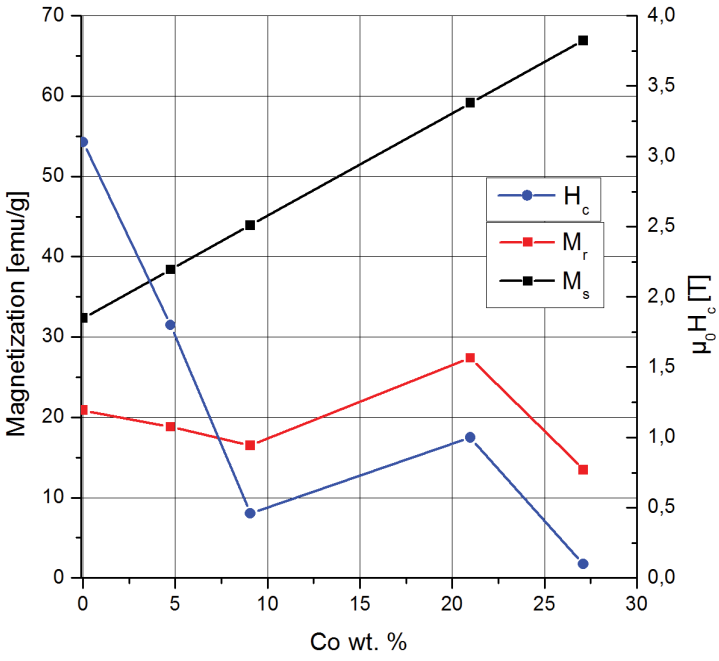

Fig. 12. Magnetic saturation M_s, magnetic remanence M_r and coercive field H_c for sintered composites, as a function of Co content

increases by about 30%) which suggests a favorable interactions between the hard and soft phases. The mechanism can be explained by the so-called spring-exchange effect. When the sintered grains of the magnetically hard and soft powders are coupled in the level of direct exchange interactions, it is possible to "join" their properties leading to an enhancement of the hard magnetic properties. In such case, the remagnetization of the soft part can be strongly influenced by the magnetic anisotropy of the hard particles in this way that the coupled object magnetically behave collectively. This lead to an increase of remanence by the magnetization of the soft part and preservation of coercivity by the hard part. A balance between the hard and soft contribution of the composite magnetization process can be determined by a derivative of magnetization, as shown in Fig. 13

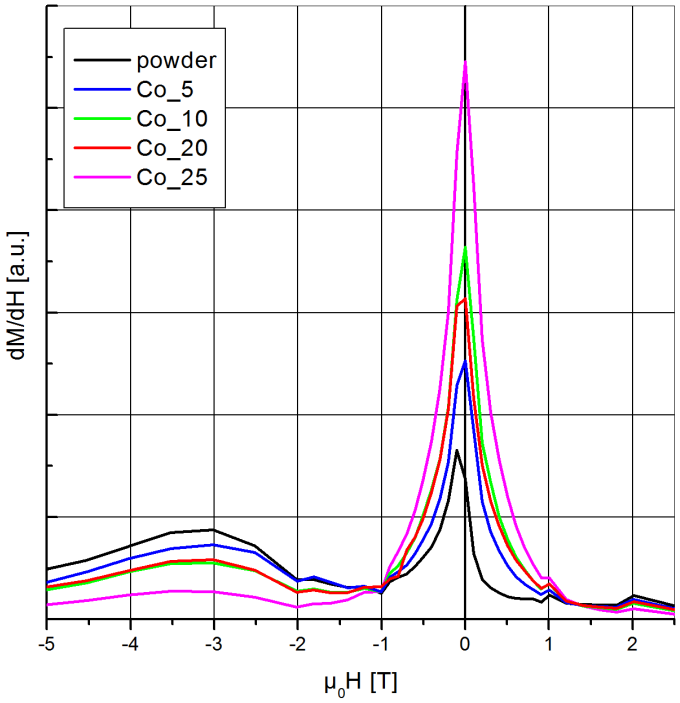

Fig. 13. Derivatives of remagnetization curves for composites with different content of Co

The area under the dM/dH curves are directly attributed to the hard/soft magnetic contribution. It should be state that for the composite Co_20, one can observe the reduced soft component in a comparison with Co_25 and even Co_10. It seems that the observed variation of the soft component contribution results from some unbounded Co particles. Apart from that, the improvement of magnetic remanence indicates a further research direction and possibility to obtaining new kind of powder composites containing magnetically soft and Fe-Nb-B-Tb ultra-high coercive phases.

4. Conclusion

The conclusions, in a reference to the $(Fe_{80}Nb_6B_{14})_{0.88}Tb_{0.12}$ powder composites, can be summarized as follows:

- the ultra-fast current aided sintering is a proper way of compacting the studied composites that preserve their hard magnetic properties,
- the applied low discharge time leads to heating mainly the grain surface, keeping the original phase structure of the sintered powder,
- the used sintering technique with the determined optimal parameters (C = 10 μF and V_Z = 1200 V) is favorable for obtaining a new kind of spring-exchange magnets containing magnetically soft and ultra-high coercive phases, as it was shown for the case of the $(Fe_{80}Nb_6B_{14})_{0.88}Tb_{0.12}$/Co powder composites.

Acknowledgement

This work was supported by the Polish National Science Center by the grant 2015/19/B/ST8/02636.

REFERENCES

[1] F.E. Luborsky, J. Appl. Phys. **37**, 1091-1094 (1966).
[2] [5] J.M.D. Coey, Scr. Mater. **67**, 524-529 (2012) .
[3] J.J. Croat, J.F. Herbst, R.W. Lee, F.E. Pinkerton, J. Appl. Phys. **55**, 2078-2081 (1984).
[4] O. Gutfleisch, J. Phys. D: Appl. Phys. **33**, R157-R172 (2000).
[5] M. Sagawa, S. Fujimura, H. Yamamoto, Y. Matsuura, IEEE. Trans. Magn. **20** (5), 1584-1589 (1984).
[6] N. Poudyal, J. Ping Liu, J. Phys. D: Appl. Phys. **46**, 043001 (23pp) (2013).
[7] [8] T. Kulik, J. Non-Cryst. Solids **287**, 145-161 (2001).
[8] A. Chrobak, G. Ziółkowski, N. Randrianantoandro, J. Alloys Comp. **583**, 48-54 (2014). DOI: 10.1016/j.jallcom.2013.08.169
[9] A. Chrobak, G. Ziółkowski, N. Randrianantoandro, J. Klimontko, D. Chrobak, K. Prusik, J. Rak. Acta Materialia **98** 318-326 (2015). DOI:10.1016/j.actamat.2015.07.056
[10] K. Granek, G. Ziółkowski, A. Chrobak, J. Klimontko, E. Talik, Acta Physica Polonica A **133** (3), 645, DOI:10.12693/APhysPolA.133.645
[11] A. Chrobak, M. Karolus, G. Haneczok, Solid State Phenom. **163**, 233-238 (2010).